Cell

CASK Functions as a Mg^{2+}-Independent Neurexin Kinase

Konark Mukherjee,[1,2,*] Manu Sharma,[1] Henning Urlaub,[3] Gleb P. Bourenkov,[5] Reinhard Jahn,[2] Thomas C. Südhof,[1,*] and Markus C. Wahl[4,6,*]

[1]Department of Neuroscience, Howard Hughes Medical Institute, University of Texas Southwestern Medical Center, 6000 Harry Hines Boulevard, Dallas, TX 75390-9111, USA

[2]Department of Neurobiology

[3]Research Group of Bioanalytical Mass Spectrometry

[4]Research Group of X-Ray Crystallography

Max-Planck-Institute for Biophysical Chemistry, Am Faßberg 11, D-37077 Göttingen, Germany

[5]EMBL Hamburg c/o Deutsches Elektronensynchrotron, Notkestraße 85, D-22603 Hamburg, Germany

[6]Georg-August-University Göttingen, Department of Medicine, Justus-von-Liebig-Weg 11, D-37077 Göttingen, Germany

*Correspondence: konark.mukherjee@utsouthwestern.edu (K.M.), thomas.sudhof@utsouthwestern.edu (T.C.S.), mwahl@gwdg.de (M.C.W.)

DOI 10.1016/j.cell.2008.02.036

SUMMARY

CASK is a unique MAGUK protein that contains an N-terminal CaM-kinase domain besides the typical MAGUK domains. The CASK CaM-kinase domain is presumed to be a catalytically inactive pseudokinase because it lacks the canonical DFG motif required for Mg^{2+} binding that is thought to be indispensable for kinase activity. Here we show, however, that CASK functions as an active protein kinase even without Mg^{2+} binding. High-resolution crystal structures reveal that the CASK CaM-kinase domain adopts a constitutively active conformation that binds ATP and catalyzes phosphotransfer without Mg^{2+}. The CASK CaM-kinase domain phosphorylates itself and at least one physiological interactor, the synaptic protein neurexin-1, to which CASK is recruited via its PDZ domain. Thus, our data indicate that CASK combines the scaffolding activity of MAGUKs with an unusual kinase activity that phosphorylates substrates recuited by the scaffolding activity. Moreover, our study suggests that other pseudokinases (10% of the kinome) could also be catalytically active.

INTRODUCTION

Protein kinases account for ≈1.7% of human genes. Ten percent of all kinases contain evolutionary changes that are thought to render them catalytically inactive, prompting them to be designated "pseudokinases" (Manning et al., 2002). Sequence analyses of these kinases revealed evolutionarily conserved alterations in otherwise highly invariant motifs. For instance, the Ca^{2+}/calmodulin-dependent (CaM)-kinase domain of CASK (Ca^{2+}/calmodulin-activated Ser-Thr kinase) is one of nine known pseudokinases, which contain alterations in the canonical Mg^{2+}-binding DFG motif that are thought to abolish catalytic activity (Boudeau et al., 2006; Manning et al., 2002).

CASK was simultaneously discovered in biochemical experiments in vertebrates because of its binding to synaptic cell-adhesion molecules called neurexins (Hata et al., 1996); in genetic experiments in *C. elegans* because it is encoded by the *Lin-2* gene that is essential for vulva development (Hoskins et al., 1996); and by sequence analyses in *D. melanogaster* because of its N-terminal CaM-kinase domain (Martin and Ollo, 1996). Deletion or mutation of *CASK* leads to anomalous synaptic function and perinatal death in mice (Atasoy et al., 2007), severe developmental deficits in *C. elegans* (Hoskins et al., 1996), and behavioral and neurotransmitter-release abnormalities in *Drosophila* (Lopes et al., 2001; Martin and Ollo, 1996; Zordan et al., 2005). In humans, the *CASK* gene has been linked to X-linked optic atrophy and mental retardation (Dimitratos et al., 1998; Froyen et al., 2007). The evolutionary conservation of CASK and the severe deletion phenotypes suggest that CASK performs important biological roles, but the precise nature of its function has remained elusive.

CASK is composed of an N-terminal CaM-kinase domain that accounts for approximately half of its primary structure and a C-terminal set of domains that is typical of MAGUKs (membrane-associated guanylate kinases), including an L27 domain, a PDZ domain, an SH3 domain, and a C-terminal guanylate kinase domain that engages in inter- and intramolecular interactions (Hsueh et al., 2000; Nix et al., 2000). Since the CASK CaM-kinase domain was presumed inactive, studies of CASK function have focused on its protein interactions. A large array of CASK interactions has been described. CASK associates stoichiometrically with Mint-1 (also called X11 or Lin-10) and Velis (also called MALS or Lin-7) (Butz et al., 1998; Borg et al., 1998). The CASK PDZ domain binds to neurexins, syndecans, and SynCAMs, putative synaptic cell-adhesion molecules (Hata et al., 1996; Cohen et al., 1998; Hsueh et al., 1998; Biederer et al., 2002). CASK also interacts with protein-4.1, and a trimeric complex composed of CASK, protein-4.1, and the cytoplasmic tail of neurexin-1 is a potent nucleator of actin polymerization (Biederer and Sudhof, 2001). CASK may bind Ca^{2+} channels (Maximov et al., 1999), K^+ channels (Leonoudakis et al., 2004), and/or the Ca^{2+} pump 4b/Cl (Schuh et al., 2003). CASK was proposed to

associate with CASKins (Tabuchi et al., 2002) and PARKIN (Fallon et al., 2002) and/or act as a nuclear transcription factor (Hsueh et al., 2000). In *C. elegans*, the CASK homolog Lin-2 mediates proper localization of the EGF receptor LET-23 (Hoskins et al., 1996). Moreover, CASK enhances Ether-a-go-go K^+ currents via increasing its phosphorylation (Marble et al., 2005). Finally, CASK may associate with CaM kinase II (CaMKII) and modulate its phosphorylation state (Hodge et al., 2006; Lu et al., 2003; Zordan et al., 2005). The regulation of phosphorylation was thought to be indirect in both the cases, as CASK was deemed a pseudokinase.

Here, we describe high-resolution crystal structures of the CaM-kinase domain of CASK complexed to different nucleotides. These structures led us to hypothesize that despite the lack of an appropriate Mg^{2+}-binding motif, CASK may nevertheless function as a protein kinase. Indeed, we show that unlike any known kinase, the CASK CaM-kinase domain catalyzes autophosphorylation and phosphotransfer to the cytoplasmic tail of neurexin-1 in the absence of Mg^{2+}. Our data suggest that CASK is unique among protein kinases in that its CaM-kinase domain uses an unusual mechanism to phosphorylate substrates that are recruited via its MAGUK component.

RESULTS

The CASK CaM-Kinase Domain Adopts a Constitutively Active Conformation

Based on sequence comparisons between the CASK CaM-kinase domain and the homologous kinases CaMKI (≈37% identity) and CaMKII (≈44% identity; Figure S1 available online), we produced a recombinant CASK CaM-kinase domain (residues 1–337; note that these residues are identical in mouse, rat, and human CASK) and determined its crystal structure. The CASK CaM-kinase domain was crystallized in two space groups, a reticularly twinned triclinic form (P1 form; Protein Data Bank (PDB) ID: 3C0G) and an orthorhombic form ($P2_12_12_1$ form; PDB ID: 3C0I). The structures of both forms were solved by molecular replacement using the coordinates of the CaMKI-kinase domain (Goldberg et al., 1996) (PDB ID: 1A06) and refined at 2.2 Å (P1 form) and 1.85 Å resolution ($P2_12_12_1$ form; Figures 1 and S3 and Table S1). The structures of the CASK CaM-kinase domain in the two crystal forms are highly similar (pairwise Cα root-mean-square deviation ≈ 0.4 Å), indicating that the overall structure was not significantly influenced by the crystalline environment (Figures 1A, 1B, S2A, and S3). Both the P1 and $P2_12_12_1$ structures exhibited uninterrupted backbone electron densities throughout the entire domain from residues 5 to 304.

The catalytic core of protein kinases can be divided into an N-terminal lobe that is involved in ATP binding and a C-terminal lobe that binds and positions the substrate in addition to contributing to ATP binding and ATP activation (Taylor et al., 2004). In the active state conformation, protein kinases adopt a similar overall fold that positions the elements in the N- and C-terminal lobes involved in substrate binding and catalysis in a canonical fashion (Huse and Kuriyan, 2002; Nolen et al., 2004). In the inactive state, in contrast, protein kinases adopt different overall folds.

The CASK CaM-kinase domain exhibits a typical protein kinase fold with an N-terminal lobe dominated by a five-stranded β sheet and an α-helical C-terminal lobe (Figures 1A, 1B, S2, and S3). Comparison of the CASK CaM-kinase domain structures with those of other protein kinases revealed that the relative orientation of N- and C-terminal lobes in the CASK CaM-kinase domain is similar to that of the active state of the death-associated protein kinase 1 (DAPK1) in a complex with the ATP analog AMPPNP (Tereshko et al., 2001) (PDB ID: 1IG1), thus resembling the catalytically active "closed conformation" (Figures 1A, 1B, 1D, and S2C). In contrast, the inactive form of CaMKI adopts a distinct "open conformation" with respect to the two lobes, resulting in a diminished affinity for nucleotides (Figures 1C and S2B) (Goldberg et al., 1996) unlike the CASK CaM-kinase domain.

Specific Structural Elements of the CASK CaM-Kinase Domain

Equivalents of all essential elements of protein kinases were found in the CASK CaM-kinase domain (Figures 1A, 1B, S2, and S3). The N-terminal lobe encompasses a Gly-rich loop (residues 19–24 in CASK; brown) and a Lys-Glu ion pair (Lys41 and Glu62 in CASK) (Figure S5C). Furthermore, it displays an optimally positioned catalytic loop (residues 141–146 in CASK; yellow) and an activation segment (green) (Figures S5A and S5B). In kinase structures corresponding to an inactive state, such as the structures of CaMKI, MnK1, and MnK2, the activation segment is often displaced from its binding site in the C-terminal lobe and frequently is disordered (Figures 1C and S2B) (Goldberg et al., 1996; Jauch et al., 2006). However, in the CASK CaM-kinase domain, the activation segment is fully ordered, and its C-terminal portion is cradled in an active state conformation within the C-terminal lobe, much like CDK2 in complex with a substrate peptide and ATP (PDB ID: 1QMZ). Superimposition of CDK2 with the CASK structure suggests that substrate peptides can bind on top of the activation segment of the CASK CaM-kinase domain oriented toward the γ-phosphate of ATP in the nucleotide-binding cleft (Figure S4B).

The C-terminal lobe of the CASK CaM-kinase domain contains an equivalent of the Mg^{2+}-binding loop. This loop is ordered in the CASK CaM-kinase domain structure (orange) as in DAPK1, while it is partially disordered in the CaMKI structure (Figures 1C and S2B). Overall, the potential catalytic elements of the CASK CaM-kinase domain could be superimposed onto corresponding elements in the DAPK1-AMPPNP cocrystal structure (Figure S2C), confirming that the structures exhibit core features and functional elements of an inherently active-state fold dissimilar to the inactive CaMKI fold.

The nucleotide-binding pocket of the CASK CaM-kinase domain was occupied by 3′-AMP in the native crystal structures (Figures 1A, 2D, S2A, and S3 and Table S1). The bound 3′-AMP is likely a byproduct of bacterial RNA degradation during protein purification. Upon soaking the crystals in 5′-AMPPNP in the presence of equimolar Mg^{2+}, the 3′-AMP could be displaced by 5′-AMPPNP, suggesting a readily accessible adenine-nucleotide-binding site (Figures 1B, 2B, and 2E, and S2A). The CASK CaM-kinase domain, thus, adopts an intrinsically active conformation amenable to nucleotide binding.

To better characterize the mode of nucleotide binding to the CASK CaM-kinase domain, we solved the structure of the best derivative crystals containing 5′-AMPPNP at 2.3 Å resolution

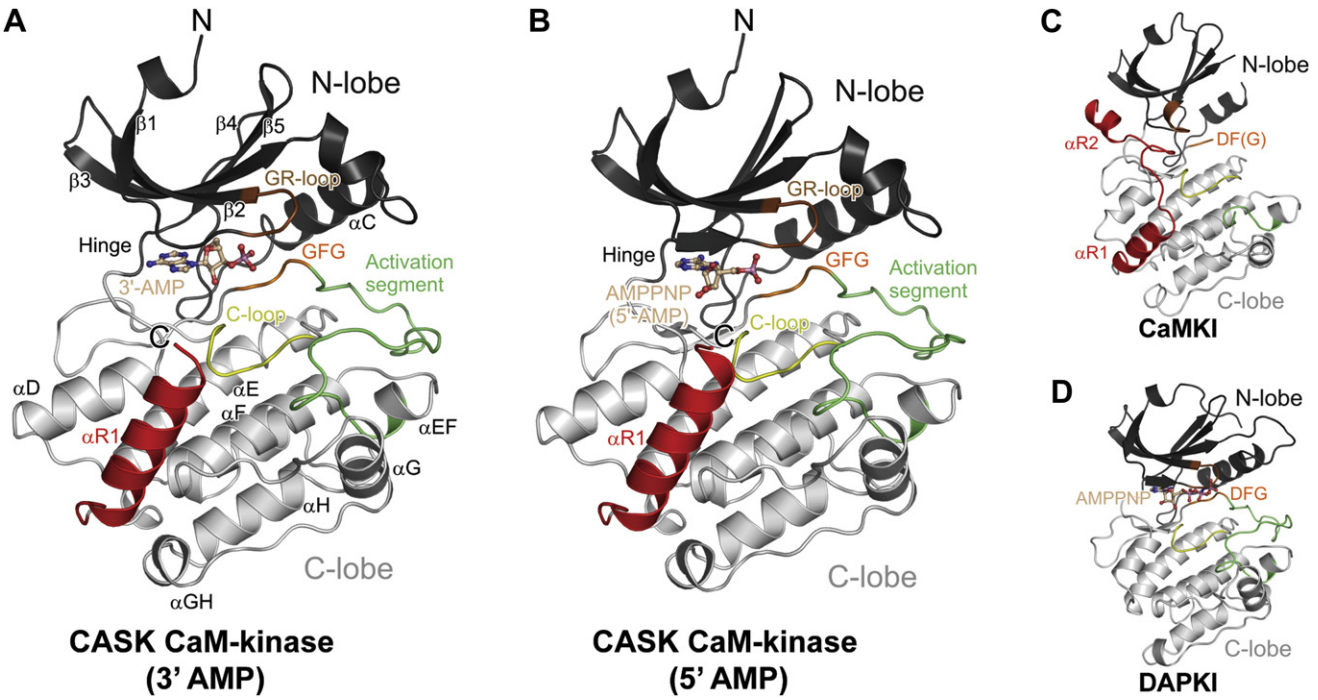

Figure 1. Structure of the CASK CaM-Kinase Domain

(A and B) Ribbon diagrams depicting the overall fold of the CASK CaM-kinase domain in a complex with 3′-AMP (orthorhombic form, A; see Figure S3 for the triclinic form) or AMPPNP (triclinic form, B).

(C and D) Ribbon diagrams of rat CaMKI (C; Goldberg et al., 1996; PDB ID: 1A06) and rat DAPK1 in a complex with Mn^{2+}-AMPPNP (D; Tereshko et al., 2001; PDB ID: 1IG1).

All structures are shown in the same orientation with the N-terminal lobes (dark gray) at the top and the C-terminal lobes (light gray) at the bottom. Specific structural elements are color-coded: portion of the glycine-rich loop (GR-loop) = brown; catalytic loop (C-loop) = yellow; D/GFG of the Mg^{2+} binding loop = orange (the third residue is disordered in the CaMKI structure); activation segment = green; C-terminal Ca^{2+}/CaM-binding segment (CaM-segment) = red. Bound nucleotides in (**A**) (3′-AMP), (B) (5′-AMP portion of AMPPNP), and (D) (AMPPNP) are shown in ball-and-sticks.

(P1 form; PDB ID: 3C0H; Table S1). The binding mode of the nucleotide in the pocket is reminiscent of the AMPPNP-bound DAPK1 structure (Tereshko et al., 2001). The N1 and N6 amino groups of the adenine form hydrogen bonds with the backbone NH of Met94 and the oxygen of Glu92, respectively. Similar to the orientation of AMPPNP in the DAPK1 structure, the adenine base of the 5′-AMP moiety was found in an *anti* conformation, and the sugar retained a C2′-*endo* conformation (Figure 2B). The overall binding and orientation of the 5′-AMP portion of the nucleotide is in agreement with the binding of ATP to generic protein kinases in an active conformation (Figures 2A–2E).

In protein kinases, bound nucleotides are coordinated by Mg^{2+} and by amino acid residues in the surrounding pocket. DAPK1 coordinates the α phosphate of AMPPNP through a hydrogen bond with Lys42. In addition, a Mg^{2+} ion (that in turn is bound to the Asp of the DFG motif and Asn of the catalytic loop) bridges the α and β phosphates (Tereshko et al., 2001) (Figure 2C). In the CASK CaM-kinase structure containing AMPPNP, the α phosphate was resolved and found to be positioned between the side chains of His145 and Lys41, without directly contacting either residue. Rather, the α phosphate is heavily hydrated and maintains water-mediated contacts to various sites in the pocket (Figures 2B and S5C). The β and γ phosphates, in contrast, were disordered; no Mg^{2+} ion could be discerned in the pocket, despite its presence in the crystallizing milieu. Thus, the structural data suggest that the CASK CaM-kinase domain is capable of coordinating ATP in a canonical orientation without Mg^{2+} and is equipped with all the structural components of a catalytic kinase, with both noticeable substitutions in the Mg^{2+}-coordinating residues (Asp162Gly of the Mg^{2+}-binding loop and Asn146Cys of the catalytic loop) and a consequential decoordination of the β and γ phosphates of ATP. These results indicate that the CASK CaM-kinase domain may bind unchelated nucleotides. To explore this hypothesis, we studied nucleotide binding to the CASK CaM-kinase domain.

ATP Binds to the CASK CaM-Kinase Domain in an Mg^{2+}-Sensitive Manner

We first tested whether the CASK CaM-kinase domain interacts with the ATP analog TNP-ATP that becomes fluorescent when inserted into the hydrophobic ATP-binding pocket (Stewart et al., 1998).

In the presence of EDTA, the CASK CaM-kinase domain induced a 3- to 5-fold increase in fluorescence intensity of TNP-ATP and a blue-shift of its emission maximum (Figure 3A). ATP titrations revealed that a 500-fold excess of ATP reduced the TNP-ATP fluorescence by 50% ($K_i^{ATP} \approx 0.365$ mM), consistent with competitive binding of ATP and TNP-ATP to a single site

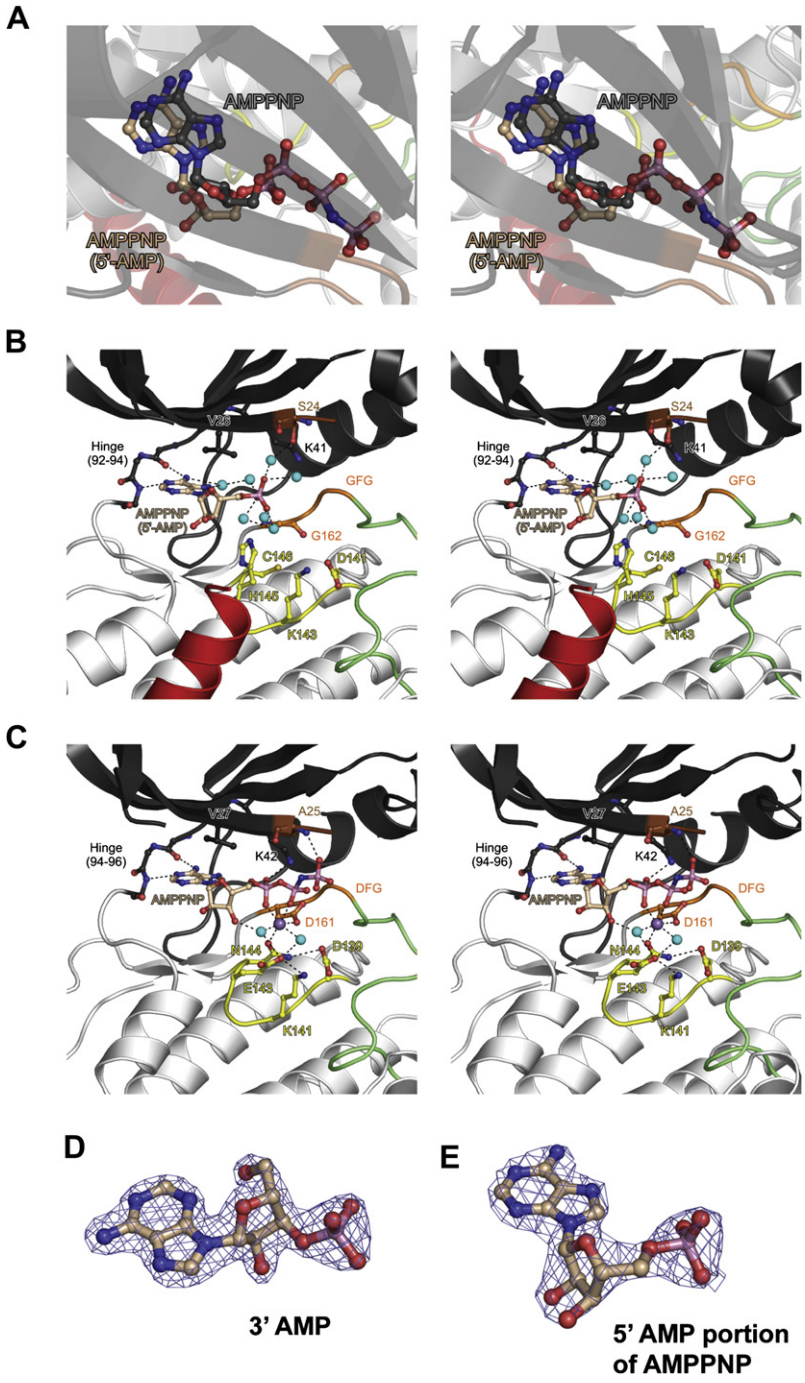

Figure 2. Architecture of the CASK CaM-Kinase Domain Nucleotide-Binding Pocket

(A) Stereo view comparing the binding of the 5′-AMP portion of AMPPNP in the present CASK structure (carbon atoms = beige) and the binding of AMPPNP as seen in a DAPK1-AMPPNP cocrystal structure (PDB ID: 1IG1; carbon atoms = gray). The nucleotides are shown after global superpositioning of the DAPK1-AMPPNP cocrystal structure onto the CASK CaM-kinase domain-AMPPNP cocrystal structure.

(B and C) Stereo plots of the nucleotide-binding pockets of the CASK (B, in complex with AMPPNP; triclinic form) and the DAPK1 CaM-kinase domains (C, in a complex with AMPPNP). Strands β1 and parts of the Gly-rich loops are removed for an unobstructed view. Portions of the Gly-rich loops (carbon = brown), the catalytic loops (carbon = yellow), the Mg^{2+}-binding loops (carbon = orange; GFG and DFG, respectively), and the nucleotides (carbon = beige) are shown as ball-and-sticks (cyan spheres = water molecules; purple sphere in DAPK1-AMPPNP = Mn^{2+} ion). Other elements are color-coded as in Figure 1. Hydrogen bonds and salt bridges are shown as dashed lines. The hinge regions (only backbone atoms are shown; residue numbers are indicated) connecting the N- and C-terminal lobes and critical residues are labeled.

(D and E) Electron densities around the bound nucleotides. $2F_o$-F_c electron density maps contoured at the 1σ level around the nucleotides bound to the CASK CaM-kinase domain are shown for the 3′-AMP of the orthorhombic crystal form (D) and the 5′-AMP portion of AMPPNP in the soaked triclinic crystal form (E). Atoms of the nucleotides are color-coded by atom type as before.

that exhibits a much higher affinity for TNP-ATP than for ATP (Stewart et al., 1998). Even a 1000-fold excess of GTP had no effect on TNP-ATP binding (Figure 3B). To further dissect the specificity of nucleotide binding to the CASK CaM-kinase domain, we examined the inhibition of TNP-ATP binding by adenine, ATP, ADP, 5′-AMP, 3′-AMP, and cAMP. Only ATP efficiently inhibited TNP-ATP binding to the CASK CaM-kinase domain, while all other tested nucleotides had little effect (Figure 3C), suggesting that the CASK CaM-kinase domain specifically binds ATP.

Since Mg^{2+} is the only divalent cation available at optimal concentration in vivo, it is invariably used as a cofactor for kinase catalysis (Waas et al., 2004). Surprisingly, however, Mg^{2+} inhibited the increase in TNP-ATP fluorescence induced by the CASK CaM-kinase domain (Figure 3A). Titrations demonstrated that the TNP-ATP–CASK CaM-kinase domain complex is diminished at higher than equimolar concentrations of Mg^{2+} ($K_i^{Mg2+} \approx 10.41$ μM), suggesting that Mg^{2+} competitively inhibits ATP binding to the CASK CaM-kinase domain (Figure S6B). Mn^{2+} and Ca^{2+} could also inhibit TNP-ATP binding (Figure 3D).

The TNP moiety of TNP-ATP could potentially form atypical contacts in the binding site (Bilwes et al., 2001), and TNP-ATP binding may not be representative of ATP binding. To address this possibility, we tested binding of the CASK CaM-kinase domain to γ^{32}P-ATP using a dot-blot assay (Figure S6A). This assay confirmed that γ^{32}P-ATP binds to the CASK CaM-kinase domain and that Mg^{2+} significantly inhibits this binding. Hence, ATP binds to the CASK CaM-kinase domain in a manner inhibited by Mg^{2+} and Ca^{2+}, consistent with the absence of the DFG motif Asp and the C-loop Asn in the CASK CaM-kinase domain.

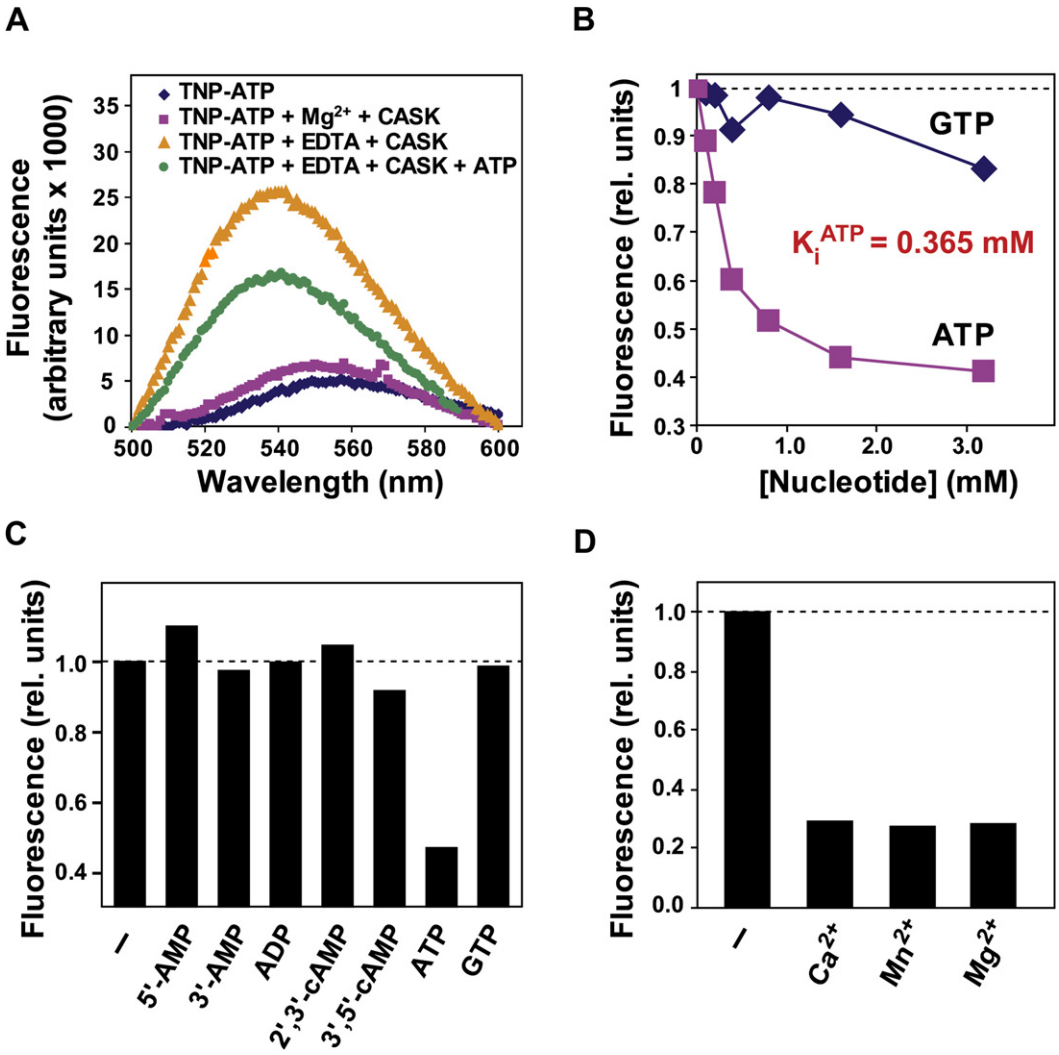

Figure 3. Nucleotide Binding by the CASK CaM-Kinase Domain: Inhibition by Divalent Ions

(A) Fluorescence emission spectra (excitation = 410 nm) of TNP-ATP (1 μM) in Tris-Cl buffer containing 2 mM $MgCl_2$ without the CASK CaM-kinase domain (blue), or after addition of the CASK CaM-kinase domain (1 μM; red), subsequent addition of EDTA (4 mM; yellow trace), and final addition of Na^+-ATP (0.5 mM; green).

(B) Titration of the TNP-ATP (1 μM) fluorescence as a function of the GTP and ATP concentration in two parallel cuvettes containing CASK CaM-kinase domain (1 μM) in Tris-Cl buffer supplemented with 4 mM EDTA (excitation = 410 nm; emission = 540 nm). Data shown represent fluorescence units after subtraction of the TNP-ATP fluorescence background, normalized to the initial reading (rel. units).

(C) Inhibition of TNP-ATP binding to the CASK CaM-kinase domain by adenine nucleotides. The fluorescence (excitation = 410 nm; emission = 540 nm) of the CASK CaM-kinase domain/TNP-ATP complex (1 μM each) was measured in EDTA (4 mM) before and after addition of the indicated nucleotides (0.5 mM). Fluorescence units were normalized after background subtraction to the respective initial readings (rel. units).

(D) Inhibition of TNP-ATP binding to the CASK CaM-kinase domain by divalent ions. The fluorescence (excitation = 410 nm; emission = 540 nm) of the CASK CaM-kinase domain/TNP-ATP complex (1 μM each) was measured in Tris-Cl buffer supplemented with EDTA (4 mM) or 2 mM of the indicated divalent cations. Data represent normalized fluorescent units (rel. units) with background subtraction. For Mg^{2+}-dependent inhibition of radioactive ATP binding, see Figure S6A. Representative data from three independent experiments are shown in each panel.

CASK CaM-Kinase Domain Is an Active Kinase

Coordination of the β and γ phosphates of ATP by Mg^{2+} ions catalyzes phosphotransfer reactions by protein kinases (Adams, 2001; Hanks and Hunter, 1995). The fact that Mg^{2+}, if anything, impairs ATP binding by the CASK CaM-kinase domain supports the notion that this domain is indeed a "pseudokinase," despite its constitutively active conformation and avid ATP binding. To test this, we examined whether the CASK CaM-kinase domain exhibits autophosphorylation activity that is typical for CaM kinases and can be employed as a test for kinase activity (Hanley et al., 1988).

The CASK CaM-kinase domain was autophosphorylated with nearly 13% efficiency independent of Mg^{2+} (Figure 4A). Tandem mass-spectrometry identified a single autophosphorylated CASK peptide containing residues 141–159 (DVKPHCVLLAS KENSAPVK; data not shown). The phosphorylated peptide is

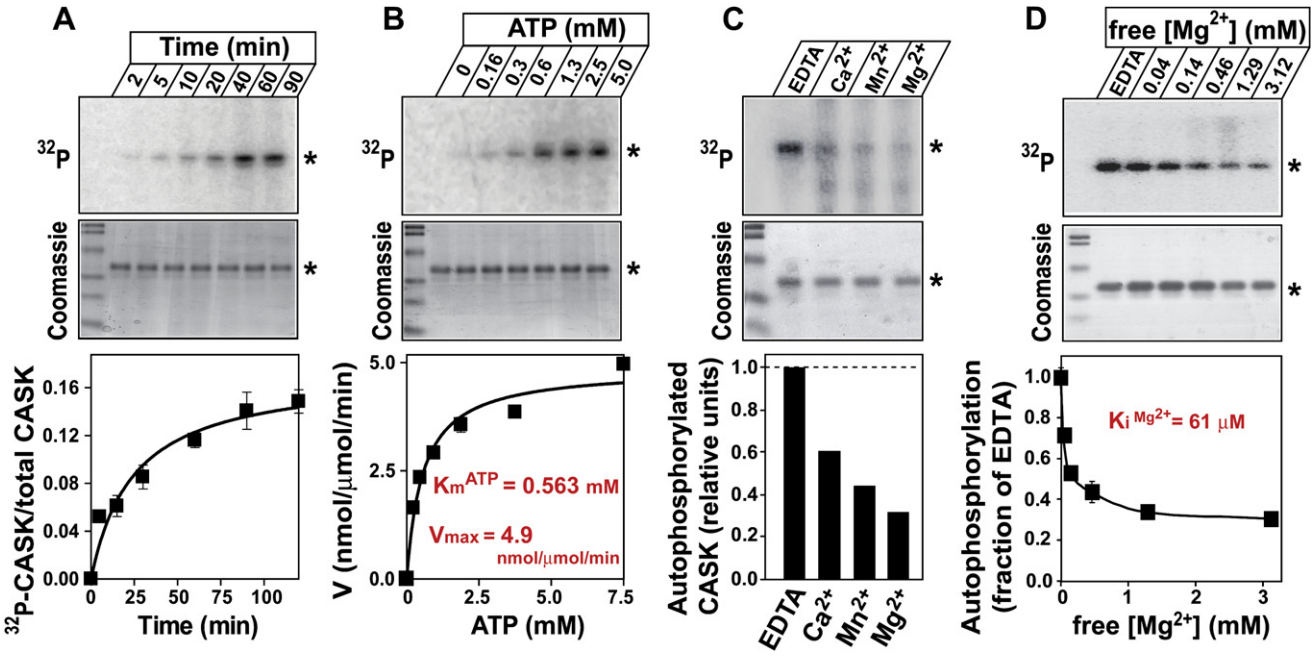

Figure 4. Autophosphorylation of the CASK CaM-Kinase Domain

All experiments were performed at room temperature with purified CASK CaM-kinase domain (1 μM) incubated with γ^{32}P-ATP (specific activity: 2 × 10^7 cpm) in Tris-Cl buffer containing 2 mM EDTA or the indicated additions. For each experiment, the upper panels depict representative autoradiograms and Coomassie stains of SDS-gels (asterisk indicates the CASK CaM-kinase domain), and the lower panels summarize CASK autophosphorylation as measured by phosphorimager. Radioactivity incorporated was calculated by relating the β counts in a band to its phosphorimager quantification and protein content. Data shown are means ± standard errors of the means (SEMs) (n = 3).

(A) Time course of CASK CaM-kinase domain autophosphorylation in 1 mM ATP.

(B) Measurement of CASK CaM-kinase domain autophosphorylation as a function of the ATP concentration for 30 min. Michaelis constant (K_m^{ATP}) and V_{max} were calculated using Graph-Pad Prism software.

(C) Decrease of CASK CaM-kinase domain autophosphorylation by divalent cations. Autophosphorylation reactions in 1 mM ATP were carried out for 30 min, in the absence of (supplemented with 2 mM EDTA) or after adding 4 mM of the indicated divalent cation.

(D) Effect of Mg^{2+} titration on CASK CaM-kinase domain autophosphorylation. Reactions were carried out in buffer supplemented with either EDTA (2 mM) or the indicated amount of free Mg^{2+} (calculated with open source software WEBMAXC).

located in a surface-exposed loop preceding the GFG motif (Figure S4A). Since the autophosphorylated peptide is remote from the substrate binding pocket, we speculate that autophosphorylation occurs in *trans*.

The autophosphorylation assay was used to calculate the Michaelis constant (K_m^{ATP}) of the CASK CaM-kinase domain for ATP (Figure 4B), revealing a K_m^{ATP} of ≈0.563 mM that is within the range of K_m^{ATP}'s for active kinases (Warmuth et al., 2007). We measured the limiting rate of autophosphorylation in experiments that approached saturation. Again, the V_{max} for autophosphorylation of the CASK CaM-kinase domain (≈4.9 nmol/μmol enzyme/min), although low, is similar to those of some other kinases, such as *Giardia lamblia* PKA (V_{max} ≈ 6.2 nmol/μmol enzyme/min; Abel et al., 2001).

Mg^{2+} and other divalent cations inhibited but did not abolish the autophosphorylation of CASK, presumably by reducing its ATP affinity (Figure 4C). Inhibition by superstoichiometric Mg^{2+} suggests that the CASK CaM-kinase domain is optimally active in the presence of unchelated free ATP, and that Mg^{2+} may regulate the kinase activity of CASK in vivo by limiting the free ATP levels in the cytosol. To examine whether catalytic phosphotransfer can occur near neuronal levels of free Mg^{2+} (0.3–0.5 mM; Taylor et al., 1991), we measured CASK autophosphorylation as a function of incrementally increased Mg^{2+} concentrations. We found that Mg^{2+} steeply inhibited the CaM-kinase domain autophosphorylation at low concentrations, but that the inhibition saturated at higher Mg^{2+} concentrations, such that a significant amount of residual autophosphorylation (>33% of maximum) remained even at very high Mg^{2+} concentrations (Figure 4D). The inhibition constant for Mg^{2+}-dependent inhibition of phosphotransfer (K_i^{Mg2+} ≈ 61 μM; Figure 4D) resembles that of the Mg^{2+}-dependent inhibition of ATP binding (K_i^{Mg2+} ≈ 10.41 μM; Figure S6B), suggesting that the inhibition of phosphotransfer by Mg^{2+} is a result of the Mg^{2+}-dependent disruption of ATP coordination. Thus, the neuronal concentration of ATP-Mg^{2+} should allow physiological catalysis by CASK, but this catalytic activity may be regulated by changes in the cytosolic divalent ion concentration.

CASK Phosphorylates Neurexin-1 In Vitro and In Vivo

CASK is abundant in brain (Hata et al., 1996) and may associate with the presynaptic active zone (Olsen et al., 2006). Since brain contains relatively low and high concentrations of free Mg^{2+} and ATP, respectively (Gotoh et al., 1999), the Mg^{2+}-dependent

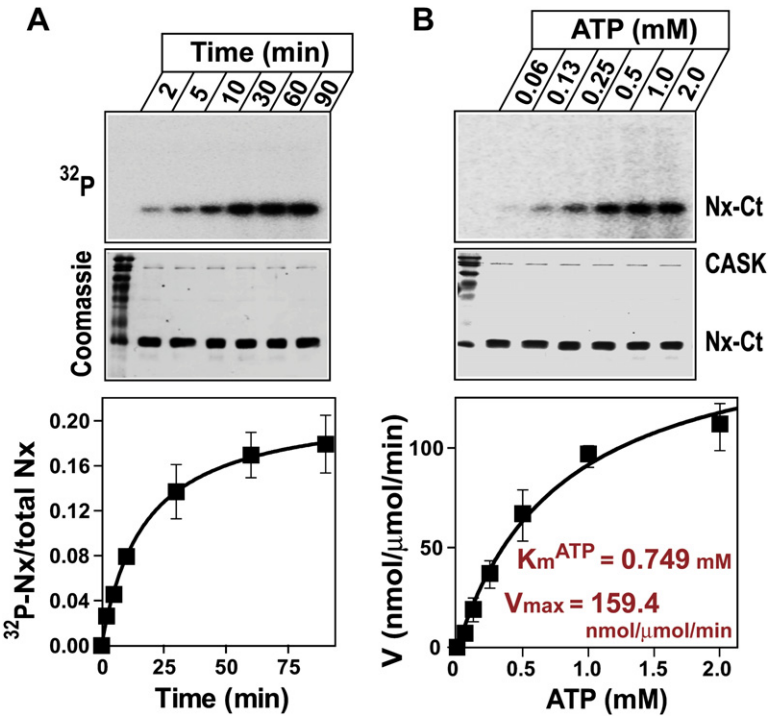

Figure 5. Full-Length CASK Phosphorylates the Cytoplasmic Tail of Neurexin-1

(A) CASK-mediated phosphorylation of the cytoplasmic tail of neurexin-1 as a function of time. Full-length CASK, bound to the GST-neurexin-1 cytoplasmic tail (Nx-Ct) immobilized on glutathione beads (in Tris-Cl buffer containing 2 mM EDTA), was incubated with γ^{32}P-ATP (2×10^7 cpm; 1 mM) at room temperature for the indicated time periods. Proteins were eluted from the beads by thrombin cleavage, separated by SDS-PAGE, and radioactivity was quantified on a phosphorimager (means ± SEMs, n = 3; corrected for protein content using Coomassie staining). Mass spectroscopy revealed that the peptides comprising residues 422–433 of neurexin-1 (QPSSAKSANKNK) were phosphorylated at one or two serine residues (data not shown). Note that the phosphorylation of the neurexin-1 cytoplasmic tail by the isolated CASK CaM-kinase domain (lacking the PDZ domain of CASK) is inefficient (Figure S7A).

(B) ATP-concentration-dependent phosphorylation of the cytoplasmic tail of neurexin-1. The complex of full-length CASK with the GST-neurexin-1 C-terminal tail protein was incubated for 30 min at room temperature in Tris-Cl buffer containing 2 mM EDTA and increasing amounts of γ^{32}P-ATP. The K_m^{ATP} and V_{max} were calculated as described in Figure 4 (means ± SEM, n = 3).

inhibition of the CASK CaM-kinase domain does not eliminate the possibility that this domain functions as a kinase. To test this, we examined whether CASK phosphorylates neurexin-1β (neurexin-1), a CASK interactor at the synapses (Hata et al., 1996).

We first investigated the in vitro phosphorylation of the cytoplasmic C-terminal tail of neurexin-1 by the isolated CASK CaM-kinase domain without the associated MAGUK domains. Although the CaM-kinase domain directly phosphorylated, in an Mg^{2+}-inhibited manner, the neurexin-1 C-tail, we observed only minimal phosphotransfer (Figure S7). Next, we investigated the ability of full-length CASK to phosphorylate neurexins because CASK binds to neurexins via its PDZ domain, suggesting that recruitment of neurexins by the CASK PDZ domain may facilitate neurexin phosphorylation. Indeed, we found that full-length CASK efficiently phosphorylated neurexin-1 (Figure 5A). These experiments were performed with a vast excess of neurexin but nevertheless resulted in a phorphorylation stoichiometry of ≈17%. CASK autophosphorylation was undetectable in these reactions, possibly due to competition with a substrate. The net rate of phosphotransfer to neurexin-1 (V_{max} ≈ 159.4 nmol/μmol enzyme/min) was 30-fold faster than the rate of CASK autophosphorylation, suggesting that neurexin, when complexed to CASK, is a substrate for the CASK CaM-kinase domain (Figures 5A and 5B). The K_m^{ATP} of neurexin-1 phosphorylation by CASK (≈748.7 μM) was similar to that of autophosphorylation reactions, consistent with the notion that ATP utilization by CASK is not enhanced by the increased availability of neurexin substrate (Figure 5B). The high phosphorylation efficiency in CASK-neurexin-1 complexes allowed phosphopeptide mapping of the neurexin-1 C-tail by LC-MS-MS. Peptides comprising residues 422–433 of neurexin-1 (QPSSAKSANKNK) were detected with single and double phosphates, establishing that the neurexin-1 C-tail is directly phosphorylated by CASK (data not shown). Consistent with a physiological neurexin phosphorylation activity of CASK, coexpression of a CASK-EGFP fusion protein with neurexin-1β in HEK293 cells recruits CASK from the cytosol to the plasma membrane and increases phosphorylation of neurexin-1β (Figures S8A and S8C). However, neurexin-1β was also phosphorylated, although to a lesser degree, without coexpression of CASK, possibly because other kinases also phosphorylate neurexin-1β.

In CASK, the L27 domain links the CaM-kinase domain to the PDZ domain, but deletion of this linker region ($CASK^{-linker}$) had no effect on neurexin phosphorylation (Figure S10). This result indicates that the L27 domain is not directly involved in CASK-mediated phosphorylation, although binding of Velis to this domain (Butz et al., 1998) may inhibit phosphorylation of a substrate bound to the PDZ domain, an exciting possibility that would provide for additional regulation of CASK activity.

Neurexin Phosphorylation by CASK Is Regulated by Neuronal Activity

We next explored whether CASK phosphorylates β-neurexins in cultured rat hippocampal neurons and detected phosphorylated β-neurexins in mature neurons at 14 days in vitro (DIV) (Figure 6A). In these experiments, we analyzed β-neurexins instead of α-neurexins because β-neurexins are easier to identify by immunoblotting than α-neurexins, but all of our conclusions also apply to α-neurexins because α- and β-neurexins contain the same cytoplasmic tail.

Cytosolic Mg^{2+} and Ca^{2+} concentrations are enhanced by synaptic activity (Gotoh et al., 1999). β-neurexin phosphorylation increased dramatically (>2-fold) when synaptic activity-driven

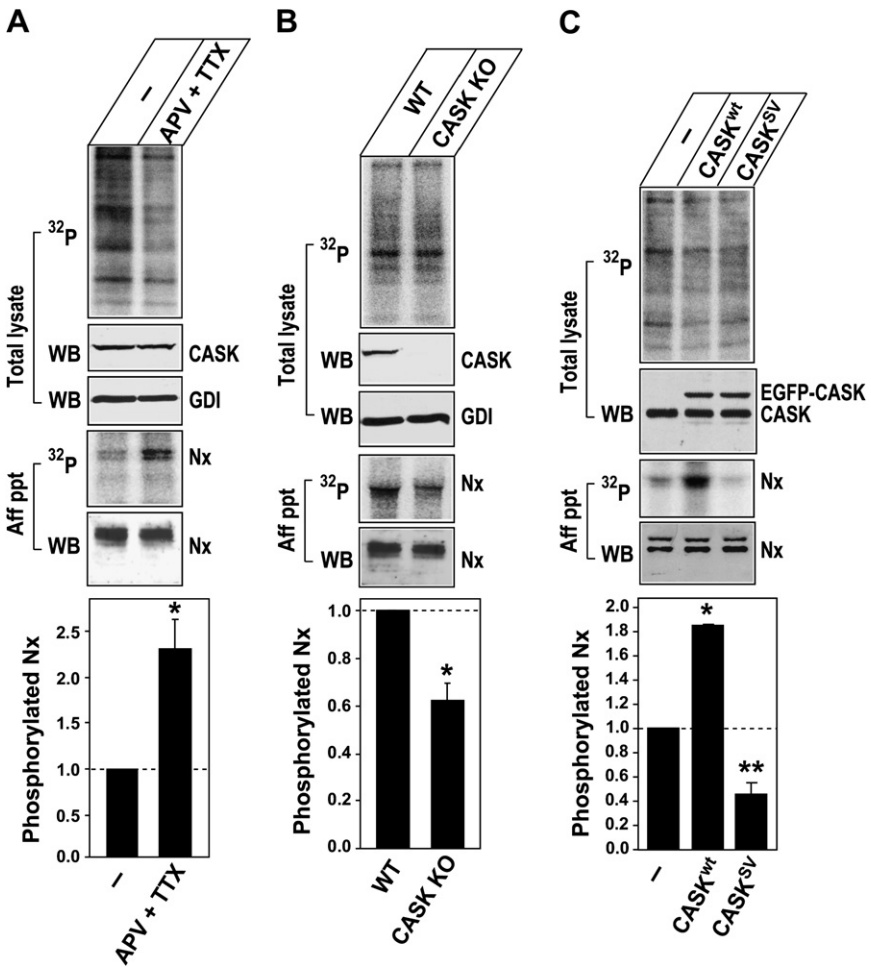

Figure 6. CASK Phosphorylates Endogenous Neurexins in Cultured Neurons

Following phosphate starvation for 30 min, neurons were incubated with 50–100 nM $^{32}P_i$ for 1 hr. Neurexins were affinity-purified (Aff ppt) from the total neuronal lysates on immobilized CASK PDZ domain, followed by separation by SDS-PAGE and immunoblotting (WB). ^{32}P-incorporation into total proteins and into β-neurexins (Nx) was visualized and quantified by phosphorimager. Lysates were also immunoblotted for CASK expression and GDI as loading controls. All neuronal cultures were incubated overnight in TTX (500 nM) and APV (50 μM) unless mentioned otherwise.

(A) Neurexin phosphorylation in neurons is increased by reducing synaptic activity, whereas total protein phosphorylation is decreased as measured by total ^{32}P-incorporation (≈58% ± 1.8%). The bar graph depicts β-neurexin phosphorylation levels in active and silenced neurons (means ± SEMs, n = 3; asterisk, p = 0.0128).

(B) Neurexin phosphorylation is reduced in CASK knockout neurons. Neurexin phosphorylation was analyzed in wild-type (WT) and acute CASK knockout (KO) mouse hippocampal cultures (DIV 10), as described above. Bar graph depicts β-neurexin phosphorylation levels in the WT and CASK KO neurons (means ± SEMs, n = 6; asterisk, p = 0.000308).

(C) Endogenous neurexin is phosphorylated by CASK. Rat hippocampal cultures (DIV 9) expressing GFP alone (–), WT EGFP-CASK fusion protein ($CASK^{wt}$), or SV mutant EGFP-CASK fusion protein ($CASK^{SV}$) were used to analyze neurexin phosphorylation, as described above. The bar graph depicts β-neurexin phosphorylation levels (means ± SEMs, n = 3; single asterisk, p = 2.9 × 10^{-5}; double asterisk, p = 0.0016).

divalent cation fluxes were suppressed with APV, a NMDA-receptor antagonist, and TTX, a Na^+-channel blocker (Figure 6A). These drugs had no effect on β-neurexin phosphorylation prior to the development of mature synapses (at 6 DIV; data not shown). Since CASK, different from other kinases, is inhibited by divalent ions, enhanced neurexin phosphorylation upon synaptic inactivation is strongly suggestive of CASK kinase activity.

To test whether CASK directly phosphorylates β-neurexin in neurons, we employed primary hippocampal cultures from CASK knockin mice that contain a floxed *CASK* gene (Atasoy et al., 2007). We acutely deleted CASK expression in these neurons using a lentivirally expressed GFP-Cre-recombinase fusion protein and found that deletion of CASK reduced β-neurexin phosphorylation by nearly 40% (Figure 6B).

Since CASK has been proposed to act as an adaptor for various molecules, including other kinases (Kaech et al., 1998; Lu et al., 2003), the deletion of CASK could have reduced phosphorylation of β-neurexins by disrupting another kinase. To test this possibility, we developed a catalytically impaired CASK mutant that could act as a dominant-negative kinase competitor when introduced into a neuron but is still expected to have normal adaptor functions. Guided by the stereochemistry of ATP coordination within the nucleotide-binding pocket of CASK (Figure 2B), we mutated Ser24 and Val26 to Asp and Leu, respectively (S24D, V26L). The CaM-kinase domain of CASK bearing this double mutation (referred to as $CASK^{SV}$) behaved as a hypomorph in vitro, as evidenced by a dramatic reduction in autophosphorylation (Figure S11A) and neurexin C-tail phosphorylation (Figure S11B). Importantly, $CASK^{SV}$ retained the ability to bind ATP (data not shown), suggesting that it still exhibits the active conformation typical of CASK and presumably still engages in native molecular interactions. In particular, $CASK^{SV}$ still binds efficiently to neurexin-1 via its PDZ domain (data not shown), thus acting as a dominant-negative competitor of the wild-type kinase.

We transfected rat hippocampal neurons at high efficiency with EGFP-fusion proteins of wild-type CASK ($CASK^{wt}$) or mutant $CASK^{SV}$ (Figure 6C). Expression of $CASK^{wt}$ produced an almost 2-fold increase in β-neurexin phosphorylation, whereas the expression of $CASK^{SV}$ caused an almost 2-fold decrease in β-neurexin phosphorylation (Figure 6C). Since the expression of $CASK^{wt}$ and the kinase hypomorph $CASK^{SV}$ assert diametrically opposite effects on the β-neurexin phosphorylation state, this phosphotransfer is likely a direct consequence of CASK kinase activity. Together, these results demonstrate that CASK physiologically phosphorylates endogenous β-neurexins

in neurons, and that this phosphorylation is regulated by the synaptic activity-driven fluxes of divalent ions.

DISCUSSION

In this study, we describe the crystal structure and biochemical properties of the CaM-kinase domain of CASK. We demonstrate that CASK functions as an active protein kinase that phosphorylates neurexins—and presumably other target proteins—by an unusual mechanism. These observations are important not only for our understanding of CASK, an enigmatic yet essential MAGUK protein with a CaM-kinase domain that is completely conserved in vertebrates, but also for our concept of "pseudokinases" in the kinome, which after all may turn out to be enzymatically active kinases with special properties.

Mg^{2+}-Independent Activity of the CASK CaM-Kinase Domain

Mg^{2+} acts as an obligate cofactor for ATP binding and phosphotransfer in all known kinases (Adams, 2001; Waas et al., 2004). Here, we demonstrate that the CASK CaM-kinase domain catalyzes phosphotransfer from ATP to proteins in the complete absence of Mg^{2+}. To our knowledge, CASK is the first kinase, indeed the first nucleotidase, known to catalyze phosphotransfers in the absence of Mg^{2+}.

The structure of the CASK CaM-kinase domain, and comparison of its structure with those of other kinases, illustrates that the CaM-kinase domain of CASK adopts a constitutively active conformation (Figures 1, 2, S2, and S3). Biochemical and enzymatic assays demonstrated that CASK binds ATP and catalyzes autophosphorylation and neurexin-1 phosphorylation in the absence of Mg^{2+} (Figures 3, 4, and 5). Compared to other kinases, CASK contains noncanonical residues in the nucleotide-binding pocket that may account for its unusual catalytic mechanism. Both of the classical metal-coordinating residues in kinases are substituted in the CASK CaM-kinase domain (Asn146Cys and Asp162Gly; see Figure S1). Moreover, Glu143 of the catalytic loop directly coordinates the metal ion in DAPK1, while in CASK, this Glu is altered to His (Glu145His). These changes likely contribute to the divalent cation-driven inhibition of the CASK CaM-kinase domain. Since the adenine base of ATP makes the most important contacts for the positioning of ATP in the nucleotide-binding pocket (Kwiatkowski and King, 1987), an altered Mg^{2+}-coordinating sequence does not exclude ATP binding and, as shown here, does not exclude catalysis. Importantly, similar to the CASK CaM-kinase domain, other pseudokinase domains with noncanonical Mg^{2+}-binding motifs may coordinate ATP and phosphorylate physiological substrates as well.

Constitutively Active CASK Kinase Is Regulated by Substrate Recruitment

CASK also differs from other CaM-kinase family members in that its CaM-kinase domain exhibits a constitutively active conformation (Figure S2). In an archetypal CaM kinase, the catalytic domain is followed by an autoinhibitory domain that inhibits kinase activity and is disinhibited by Ca^{2+}/calmodulin binding (Goldberg et al., 1996). The CASK CaM-kinase domain is followed by a sequence that is homologous to the autoinhibitory domain of CaM kinases (Figure S1) and that also binds Ca^{2+}/calmodulin (Hata et al., 1996). However, unlike typical CaM kinases, the autoinhibitory helix (αR1) of CASK does not engage in direct contacts with the ATP-binding cleft (Figures 1 and S3). We also did not discern evidence for further C-terminal residues interacting with the ATP-binding cleft, as in CaMKI, and we detected no stimulatory effect of Ca^{2+} and/or calmodulin on the CASK kinase activity (data not shown). Thus, the CASK CaM-kinase domain appears to retain a nonfunctional autoinhibitory domain as an evolutionary vestige of CaM kinases. CASK, therefore, differs from other, evolutionarily closely related CaM-kinase domains not only in its Mg^{2+} independence but also in its inherently "closed" active conformation that constitutively binds nucleotides.

An almost essential consequence of the constitutively active conformation of the CASK CaM-kinase domain is that the domain exhibits a very low catalytic rate, as shown in autophosphorylation measurements (Figure 4) and in measurements of neurexin-1 phosphorylation by the isolated CASK CaM-kinase domain lacking the neurexin-binding PDZ domain of CASK (Figure S7). Mechanistically, this low rate is likely due to the loss of Mg^{2+} coordination by the domain. The low catalytic rate of the CASK CaM-kinase domain presumably serves to ensure that the kinase does not phosphorylate potential substrates randomly. We show that the phosphorylation rate of neurexin-1 is increased dramatically, however, when full-length CASK forms a complex with neurexin-1 via the CASK PDZ domain (Figure 5). This result suggests a general mechanism for CASK kinase activity, whereby CASK couples an intrinsically slow but constitutively active kinase domain to a PDZ domain that recruits the substrates to the kinase domain, thereby increasing the local substrate concentration by many orders of magnitude (see model in Figure 7). According to this model, CASK unites two separate functions—the recruitment activity of MAGUKs and the kinase activity of the CaM-kinase domain—into a single unit whose objective is phosphorylation of specific interacting proteins (Figure 7).

Physiological Implications

CASK phosphorylates neurexin-1 in vitro and in vivo in a reaction that depends on a catalytically active CaM-kinase domain (Figures 5 and 6). Neurexin, described here as a substrate of CASK, is a presynaptic cell-adhesion molecule (Nam and Chen, 2005; Ushkaryov et al., 1992; reviewed in Missler et al., 2003). Its heterotypic binding to postsynaptic neuroligins may be involved in synaptic function and could induce synapse formation even on non-neuronal cocultured cells (Graf et al., 2004). The neurexin-neuroligin interaction is a candidate for synaptic specialization and pre-post-synapse communication. Both neurexin and neuroligin mutations have been linked to autism spectrum disorders (Jamain et al., 2003; Szatmari et al., 2007). Deletion of CASK may be connected to X-linked optic atrophy and mental retardation (Dimitratos et al., 1998; Froyen et al., 2007). The evolutionary conservation of CASK and neurexins, and their central importance for survival and synaptic function in mice (Atasoy et al., 2007; Missler et al., 2003), indicate that neurexin phosphorylation by CASK may be crucial to neuronal function.

In addition to the control of CASK kinase activity by the PDZ-domain-mediated substrate recruitment, we examined whether

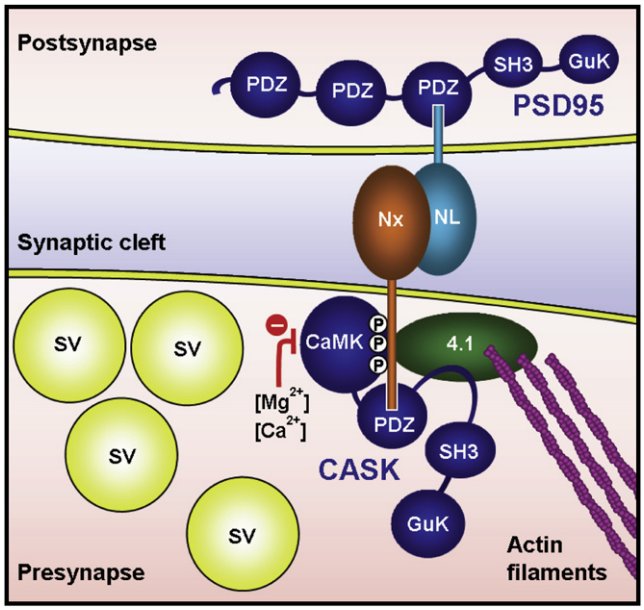

Figure 7. Model of Neurexin Phosphorylation by CASK

Neurexin (Nx) and neuroligin (NL) are thought to interact extracellularly with each other across the synaptic cleft and to associate intracellularly with the MAGUKs CASK and PSD-95, respectively. CASK is recruited to the cytosolic C-tail of neurexin via the CASK PDZ domain and phosphorylates the neurexin C-terminal tail. Protein 4.1, which binds the C-tail of neurexin as well as CASK, nucleates actin filaments, modulating the presynaptic cytoskeleton. The red indicator depicts the inhibition of CASK CaM-kinase activity due to an increase in cytosolic divalent cations.

it is regulated by synaptic activity-driven rises in Ca^{2+} and Mg^{2+} levels. In neurons, synaptic activity triggers a surge in Mg^{2+} and Ca^{2+} levels (Gotoh et al., 1999) that could regulate CASK kinase activity. Indeed, we observed a strong increase in neurexin phosphorylation upon silencing synapses in mature neurons, indicating that contrary to other kinases, CASK kinase is inhibited by neuronal activity (Figure 6A). We envision that CASK kinase activity is maximal during neuronal development and synaptogenesis and declines with the onset of synaptic function but is reactivated when neurons are silenced. This developmentally regulated activity is in line with the phenotypic defects in CASK knockout mice (Atasoy et al., 2007) as well as the developmental nature of CASK- and neurexin-related pathologies (Froyen et al., 2007; Szatmari et al., 2007).

CASK is expressed ubiquitously at low levels (Hata et al., 1996). The non-neuronal functions of CASK are evident from developmental defects in CASK/Lin-2 null animals, such as cleft palate in mice (Atasoy et al., 2007) and vulval dysgenesis in *C. elegans* (Hoskins et al., 1996). In non-neuronal cells, CASK-interacting adhesion molecules of the syndecan or JAM families could be substrates (Cohen et al., 1998; Hsueh et al., 1998; Martinez-Estrada et al., 2001). These molecules share the PDZ-domain-mediated CASK association, and at least in the case of syndecan-2, serine residues in the cytoplasmic tail homologous to those of neurexins are phosphorylated in vivo (Itano et al., 1996).

Finally, of the 518 known kinases in the human genome, 48 are predicted to be pseudokinases (Boudeau et al., 2006). In each of these pseudokinases, one or more of the invariant motifs are altered. Nine of the presumed pseudokinases, including CASK, lack a canonical DFG motif. Furthermore, this motif is altered along with other canonical motifs (HRD and/or VAIK) in 22 additional pseudokinases. Our data on CASK suggest that other pseudokinases, especially those with atypical DFG motifs, could be active in physiologically relevant environments, indicating that the catalytically active kinome may be more diverse than originally envisioned.

EXPERIMENTAL PROCEDURES

Detailed experimental procedures are found in the Supplemental Data.

TNP-ATP Binding Assay

Fluorescence measurements of TNP-ATP (from Molecular Probes Inc; Eugene, OR, USA) were obtained in Tris-Cl buffer (50 mM Tris-HCl, pH 7.2, 50 mM KCl) in 1 cm × 1 cm fluorescence cuvettes at 25°C using a Jobin Yvon-Spex Fluoromax-2 (Stewart et al., 1998). Samples were excited at 410 nm, and emission was recorded at 540 nm or scanned from 500–600 nm. Signal from a TNP-ATP buffer control, in which BSA replaced CASK CaM-kinase domain, was subtracted as background.

In Vitro Phosphorylation Assays

All assays were performed in Tris-Cl buffer containing 2 mM EDTA or the divalent cations indicated. Briefly, immobilized GST-fusion proteins (either the GST-CASK CaM-kinase domain or the GST-neurexin C-tail complexed to CASK) were incubated with 1 mM γ^{32}P-ATP (specific activity: 2 × 10^7 cpm) for 1 hr at room temperature. For determining the K_m^{ATP}, the GST-fusion proteins were incubated with increasing concentration of ATP for 30 min. After washing in Tris-Cl buffer, proteins were eluted from the beads by thrombin cleavage, separated by SDS-PAGE, and visualized on a phosphorimager and by Coomassie staining. Radioactivity incorporated was calculated by correlating the β counts in a band (measured with Beckman-Coulter LS-6000 scintillation system) with its phosphorimager quantification (performed with Molecular Dynamics Storm scanner and Image-Quant software).

In Vivo Kinase Activity Assays

Dissociated hippocampal cultures at the indicated DIVs were kept in 0.5 μM TTX and 50 μM APV overnight, washed, and incubated in phosphate-free depletion buffer (10 mM HEPES-NaOH, pH 7.2, 150 mM NaCl, 4 mM KCl, 2 mM $MgCl_2$, 2 mM $CaCl_2$, 10 mM D-glucose, 100 nM insulin) for 30 min at 37°C, followed by incubation in the same buffer supplemented with 100 μCi $^{32}P_i$ for 1 hr. Cells were washed twice with phosphate-free buffer and lysed in ice-cold solubilization buffer (10 mM Tris-Cl, pH 6.8, 150 mM NaCl, 1% Triton X-100, 4 mM EDTA), supplemented with protease inhibitor cocktail and phosphatase inhibitor cocktails-1 and -2 (Sigma). Debris was spun down (14,000 rpm for 10 min at 4°C) and supernatant was incubated with immobilized GST-CASK PDZ domain overnight. Complexes were washed in solubilization buffer and separated by SDS-PAGE, followed by phosphorimager scanning. β-neurexin immunoblots were used as loading control. Neuronal lysates were also separated and immunoblotted with CASK monoclonal antibody (Transduction Labs).

SUPPLEMENTAL DATA

Supplemental Data include one table, thirteen figures, and detailed Supplemental Experimental Procedures and can be found with this article online at http://www.cell.com/cgi/content/full/133/2/328/DC1/.

ACKNOWLEDGMENTS

We thank Drs. Elizabeth Goldsmith, A.J. Robison, Mark Etherton, Gottfried Mieskes, Antony Boucard, and Ralf Jauch for comments on the manuscript; Lin Fan, Andrea Roth, and Izabella Kornblum for technical support; Reinhard Lührmann for the use of crystallography equipment; and the staff at beamlines

BW6, DESY, Hamburg, Germany and PX2, SLS, Villigen, Switzerland for support during diffraction data collection. This work was supported by a grant from the NIMH (R37 MH52804-08 to T.C.S.) and the Max-Planck-Society (M.C.W.). M.S. is a Human Frontiers Long Term Fellow.

Received: July 9, 2007
Revised: October 30, 2007
Accepted: February 6, 2008
Published: April 17, 2008

REFERENCES

Abel, E.S., Davids, B.J., Robles, L.D., Loflin, C.E., Gillin, F.D., and Chakrabarti, R. (2001). Possible roles of protein kinase A in cell motility and excystation of the early diverging eukaryote Giardia lamblia. J. Biol. Chem. *276*, 10320–10329.

Adams, J.A. (2001). Kinetic and catalytic mechanisms of protein kinases. Chem. Rev. *101*, 2271–2290.

Atasoy, D., Schoch, S., Ho, A., Nadasy, K.A., Liu, X., Zhang, W., Mukherjee, K., Nosyreva, E.D., Fernandez-Chacon, R., Missler, M., et al. (2007). Deletion of CASK in mice is lethal and impairs synaptic function. Proc. Natl. Acad. Sci. USA *104*, 2525–2530.

Biederer, T., Sara, Y., Mozhayeva, M., Atasoy, D., Liu, X., Kavalali, E.T., and Sudhof, T.C. (2002). SynCAM, a synaptic adhesion molecule that drives synapse assembly. Science *297*, 1525–1531.

Biederer, T., and Sudhof, T.C. (2001). CASK and protein 4.1 support F-actin nucleation on neurexins. J. Biol. Chem. *276*, 47869–47876.

Bilwes, A.M., Quezada, C.M., Croal, L.R., Crane, B.R., and Simon, M.I. (2001). Nucleotide binding by the histidine kinase CheA. Nat. Struct. Biol. *8*, 353–360.

Borg, J.P., Straight, S.W., Kaech, S.M., de Taddeo-Borg, M., Kroon, D.E., Karnak, D., Turner, R.S., Kim, S.K., and Margolis, B. (1998). Identification of an evolutionarily conserved heterotrimeric protein complex involved in protein targeting. J. Biol. Chem. *273*, 31633–31636.

Boudeau, J., Miranda-Saavedra, D., Barton, G.J., and Alessi, D.R. (2006). Emerging roles of pseudokinases. Trends Cell Biol. *16*, 443–452.

Butz, S., Okamoto, M., and Sudhof, T.C. (1998). A tripartite protein complex with the potential to couple synaptic vesicle exocytosis to cell adhesion in brain. Cell *94*, 773–782.

Cohen, A.R., Woods, D.F., Marfatia, S.M., Walther, Z., Chishti, A.H., and Anderson, J.M. (1998). Human CASK/LIN-2 binds syndecan-2 and protein 4.1 and localizes to the basolateral membrane of epithelial cells. J. Cell Biol. *142*, 129–138.

Dimitratos, S.D., Stathakis, D.G., Nelson, C.A., Woods, D.F., and Bryant, P.J. (1998). The location of human CASK at Xp11.4 identifies this gene as a candidate for X-linked optic atrophy. Genomics *51*, 308–309.

Fallon, L., Moreau, F., Croft, B.G., Labib, N., Gu, W.J., and Fon, E.A. (2002). Parkin and CASK/LIN-2 associate via a PDZ-mediated interaction and are co-localized in lipid rafts and postsynaptic densities in brain. J. Biol. Chem. *277*, 486–491.

Froyen, G., Van Esch, H., Bauters, M., Hollanders, K., Frints, S.G., Vermeesch, J.R., Devriendt, K., Fryns, J.P., and Marynen, P. (2007). Detection of genomic copy number changes in patients with idiopathic mental retardation by high-resolution X-array-CGH: important role for increased gene dosage of XLMR genes. Hum. Mutat. *28*, 1034–1042.

Goldberg, J., Nairn, A.C., and Kuriyan, J. (1996). Structural basis for the autoinhibition of calcium/calmodulin-dependent protein kinase I. Cell *84*, 875–887.

Gotoh, H., Kajikawa, M., Kato, H., and Suto, K. (1999). Intracellular Mg2+ surge follows Ca2+ increase during depolarization in cultured neurons. Brain Res. *828*, 163–168.

Graf, E.R., Zhang, X., Jin, S.X., Linhoff, M.W., and Craig, A.M. (2004). Neurexins induce differentiation of GABA and glutamate postsynaptic specializations via neuroligins. Cell *119*, 1013–1026.

Hanks, S.K., and Hunter, T. (1995). Protein kinases 6. The eukaryotic protein kinase superfamily: kinase (catalytic) domain structure and classification. FASEB J. *9*, 576–596.

Hanley, R.M., Means, A.R., Kemp, B.E., and Shenolikar, S. (1988). Mapping of calmodulin-binding domain of Ca2+/calmodulin-dependent protein kinase II from rat brain. Biochem. Biophys. Res. Commun. *152*, 122–128.

Hata, Y., Butz, S., and Sudhof, T.C. (1996). CASK: a novel dlg/PSD95 homolog with an N-terminal calmodulin-dependent protein kinase domain identified by interaction with neurexins. J. Neurosci. *16*, 2488–2494.

Hodge, J.J., Mullasseril, P., and Griffith, L.C. (2006). Activity-dependent gating of CaMKII autonomous activity by *Drosophila* CASK. Neuron *51*, 327–337.

Hoskins, R., Hajnal, A.F., Harp, S.A., and Kim, S.K. (1996). The C. elegans vulval induction gene lin-2 encodes a member of the MAGUK family of cell junction proteins. Development *122*, 97–111.

Hsueh, Y.P., Yang, F.C., Kharazia, V., Naisbitt, S., Cohen, A.R., Weinberg, R.J., and Sheng, M. (1998). Direct interaction of CASK/LIN-2 and syndecan heparan sulfate proteoglycan and their overlapping distribution in neuronal synapses. J. Cell Biol. *142*, 139–151.

Hsueh, Y.P., Wang, T.F., Yang, F.C., and Sheng, M. (2000). Nuclear translocation and transcription regulation by the membrane-associated guanylate kinase CASK/LIN-2. Nature *404*, 298–302.

Huse, M., and Kuriyan, J. (2002). The conformational plasticity of protein kinases. Cell *109*, 275–282.

Itano, N., Oguri, K., Nagayasu, Y., Kusano, Y., Nakanishi, H., David, G., and Okayama, M. (1996). Phosphorylation of a membrane-intercalated proteoglycan, syndecan-2, expressed in a stroma-inducing clone from a mouse Lewis lung carcinoma. Biochem. J. *315*, 925–930.

Jamain, S., Quach, H., Betancur, C., Rastam, M., Colineaux, C., Gillberg, I.C., Soderstrom, H., Giros, B., Leboyer, M., Gillberg, C., et al. (2003). Mutations of the X-linked genes encoding neuroligins NLGN3 and NLGN4 are associated with autism. Nat. Genet. *34*, 27–29.

Jauch, R., Cho, M.K., Jakel, S., Netter, C., Schreiter, K., Aicher, B., Zweckstetter, M., Jackle, H., and Wahl, M.C. (2006). Mitogen-activated protein kinases interacting kinases are autoinhibited by a reprogrammed activation segment. EMBO J. *25*, 4020–4032.

Kaech, S.M., Whitfield, C.W., and Kim, S.K. (1998). The LIN-2/LIN-7/LIN-10 complex mediates basolateral membrane localization of the C. elegans EGF receptor LET-23 in vulval epithelial cells. Cell *94*, 761–771.

Kwiatkowski, A.P., and King, M.M. (1987). Mapping of the adenosine 5′-triphosphate binding site of type II calmodulin-dependent protein kinase. Biochemistry *26*, 7636–7640.

Leonoudakis, D., Conti, L.R., Radeke, C.M., McGuire, L.M., and Vandenberg, C.A. (2004). A multiprotein trafficking complex composed of SAP97, CASK, Veli, and Mint1 is associated with inward rectifier Kir2 potassium channels. J. Biol. Chem. *279*, 19051–19063.

Lopes, C., Gassanova, S., Delabar, J.M., and Rachidi, M. (2001). The CASK/Lin-2 Drosophila homologue, Camguk, could play a role in epithelial patterning and in neuronal targeting. Biochem. Biophys. Res. Commun. *284*, 1004–1010.

Lu, C.S., Hodge, J.J., Mehren, J., Sun, X.X., and Griffith, L.C. (2003). Regulation of the Ca2+/CaM-responsive pool of CaMKII by scaffold-dependent autophosphorylation. Neuron *40*, 1185–1197.

Manning, G., Whyte, D.B., Martinez, R., Hunter, T., and Sudarsanam, S. (2002). The protein kinase complement of the human genome. Science *298*, 1912–1934.

Marble, D.D., Hegle, A.P., Snyder, E.D., 2nd, Dimitratos, S., Bryant, P.J., and Wilson, G.F. (2005). Camguk/CASK enhances Ether-a-go-go potassium current by a phosphorylation-dependent mechanism. J. Neurosci. *25*, 4898–4907.

Martin, J.R., and Ollo, R. (1996). A new Drosophila Ca2+/calmodulin-dependent protein kinase (Caki) is localized in the central nervous system and implicated in walking speed. EMBO J. *15*, 1865–1876.

Martinez-Estrada, O.M., Villa, A., Breviario, F., Orsenigo, F., Dejana, E., and Bazzoni, G. (2001). Association of junctional adhesion molecule with

calcium/calmodulin-dependent serine protein kinase (CASK/LIN-2) in human epithelial caco-2 cells. J. Biol. Chem. *276*, 9291–9296.

Maximov, A., Sudhof, T.C., and Bezprozvanny, I. (1999). Association of neuronal calcium channels with modular adaptor proteins. J. Biol. Chem. *274*, 24453–24456.

Missler, M., Zhang, W., Rohlmann, A., Kattenstroth, G., Hammer, R.E., Gottmann, K., and Sudhof, T.C. (2003). Alpha-neurexins couple Ca2+ channels to synaptic vesicle exocytosis. Nature *423*, 939–948.

Nam, C.I., and Chen, L. (2005). Postsynaptic assembly induced by neurexin-neuroligin interaction and neurotransmitter. Proc. Natl. Acad. Sci. USA *102*, 6137–6142.

Nix, S.L., Chishti, A.H., Anderson, J.M., and Walther, Z. (2000). hCASK and hDlg associate in epithelia, and their src homology 3 and guanylate kinase domains participate in both intramolecular and intermolecular interactions. J. Biol. Chem. *275*, 41192–41200.

Nolen, B., Taylor, S., and Ghosh, G. (2004). Regulation of protein kinases; controlling activity through activation segment conformation. Mol. Cell *15*, 661–675.

Olsen, O., Moore, K.A., Nicoll, R.A., and Bredt, D.S. (2006). Synaptic transmission regulated by a presynaptic MALS/Liprin-alpha protein complex. Curr. Opin. Cell Biol. *18*, 223–227.

Schuh, K., Uldrijan, S., Gambaryan, S., Roethlein, N., and Neyses, L. (2003). Interaction of the plasma membrane Ca2+ pump 4b/CI with the Ca2+/calmodulin-dependent membrane-associated kinase CASK. J. Biol. Chem. *278*, 9778–9783.

Stewart, R.C., VanBruggen, R., Ellefson, D.D., and Wolfe, A.J. (1998). TNP-ATP and TNP-ADP as probes of the nucleotide binding site of CheA, the histidine protein kinase in the chemotaxis signal transduction pathway of Escherichia coli. Biochemistry *37*, 12269–12279.

Szatmari, P., Paterson, A.D., Zwaigenbaum, L., Roberts, W., Brian, J., Liu, X.Q., Vincent, J.B., Skaug, J.L., Thompson, A.P., Senman, L., et al. (2007). Mapping autism risk loci using genetic linkage and chromosomal rearrangements. Nat. Genet. *39*, 319–328.

Tabuchi, K., Biederer, T., Butz, S., and Sudhof, T.C. (2002). CASK participates in alternative tripartite complexes in which Mint 1 competes for binding with caskin 1, a novel CASK-binding protein. J. Neurosci. *22*, 4264–4273.

Taylor, J.S., Vigneron, D.B., Murphy-Boesch, J., Nelson, S.J., Kessler, H.B., Coia, L., Curran, W., and Brown, T.R. (1991). Free magnesium levels in normal human brain and brain tumors: 31P chemical-shift imaging measurements at 1.5 T. Proc. Natl. Acad. Sci. USA *88*, 6810–6814.

Taylor, S.S., Yang, J., Wu, J., Haste, N.M., Radzio-Andzelm, E., and Anand, G. (2004). PKA: a portrait of protein kinase dynamics. Biochim. Biophys. Acta *1697*, 259–269.

Tereshko, V., Teplova, M., Brunzelle, J., Watterson, D.M., and Egli, M. (2001). Crystal structures of the catalytic domain of human protein kinase associated with apoptosis and tumor suppression. Nat. Struct. Biol. *8*, 899–907.

Ushkaryov, Y.A., Petrenko, A.G., Geppert, M., and Sudhof, T.C. (1992). Neurexins: synaptic cell surface proteins related to the alpha-latrotoxin receptor and laminin. Science *257*, 50–56.

Waas, W.F., Rainey, M.A., Szafranska, A.E., Cox, K., and Dalby, K.N. (2004). A kinetic approach towards understanding substrate interactions and the catalytic mechanism of the serine/threonine protein kinase ERK2: identifying a potential regulatory role for divalent magnesium. Biochim. Biophys. Acta *1697*, 81–87.

Warmuth, M., Kim, S., Gu, X.J., Xia, G., and Adrian, F. (2007). Ba/F3 cells and their use in kinase drug discovery. Curr. Opin. Oncol. *19*, 55–60.

Zordan, M.A., Massironi, M., Ducato, M.G., Te Kronnie, G., Costa, R., Reggiani, C., Chagneau, C., Martin, J.R., and Megighian, A. (2005). Drosophila CAKI/CMG protein, a homolog of human CASK, is essential for regulation of neurotransmitter vesicle release. J. Neurophysiol. *94*, 1074–1083.